Functional Materials 16, No.2 (2009)

Structure, phase states and change of magnetic properties at recrystallization of thin-film Ni laser condensates

A.G.Bagmut, I.G.Shipkova, V.A.Zhuchkov

National Technical University "Kharkiv Polytechnic of Institute",
21 Frunze St., 61002 Kharkiv, Ukraine

Received November 5, 2008

The influence of a substrate temperature and of oxygen pressure in the evaporation chamber on the structure and phase state of nickel laser condensates has been studied by electron microscopy. The regularities of structure-phase transformations in the films and changes of magnetic properties after annealing have been investigated. It is established that a wide spectrum of thin-film states can be provided by varying the oxygen pressure in the evaporation chamber and the substrate temperature during nickel condensation. Amorphous Ni films are formed as well those with metastable HCP lattice (α phase), with stable GCC lattice (β phase), and NiO films with FCC structure. The effective activation energy value for the processes controlling the formation of α phase of Ni grains makes about 0.26 eV/atom. Annealing of amorphous films initiates their crystallization with formation of disordered precipitates of β phase of nickel. Annealing of Ni films with metastable HCP lattice initiates the HCP → FCC polymorphic transformation accompanied by sharp increase of grain size and changes in its magnetic properties. The annealed films get a magnetic moment and hysteresis is observed at magnetization reversal.

Проведено электронно-микроскопическое исследование влияния температуры подложки и давления кислорода в испарительной камере на структуру и фазовый состав лазерных конденсатов никеля. Изучены закономерности структурно-фазовых трансформаций и изменение магнитных свойств пленок после отжига. Установлено, что варьированием давления кислорода в испарительной камере и температуры подложки в процессе конденсации никеля можно обеспечить формирование широкого спектра тонкопленочных состояний. Конденсируются аморфные пленки Ni, пленки Ni с метастабильной ГПУ решеткой (α фаза), пленки Ni со стабильной ГЦК решеткой (β фаза) и пленки оксида NiO со структурой ГЦК. Эффективное значение энергии активации процессов, контролирующих образование зерен α фазы Ni, составляет ~ 0,26 эВ/атом. Отжиг аморфных пленок инициирует их кристаллизацию с образованием разориентированных выделений β фазы никеля. Отжиг пленок Ni с метастабильной ГПУ решеткой инициирует полиморфное превращение ГПУ → ГЦК, которое сопровождается резким увеличением размера зерен и изменением магнитных характеристик пленки. В результате отжига пленки приобретают магнитный момент, а при перемагничивании имеет место гистерезис.

Investigation of structure, phase state, and properties of thin nanocrystalline Ni films is of both fundamental and practical interest. These films belong to solid low-dimensional materials and are used in modern microelectronics as miniature functional elements and in magnetic memory systems as interference filters, reflecting and anti-reflecting coatings [1]. To provide the required electro-physical properties of thin film structures, it is necessary to advance the technologies of their preparation.

The pulsed laser deposition (PLD) in vacuum or in controlled gas medium is one way to solve this problem. In [2], the diagram is presented showing the phase states of deposited films depending on the ratio of gas flow to metal vapor one hitting the film growth surface. Absorption and chemical activity of metal are considered, too. However, the above-mentioned diagram does not include any data concerning the PLD of nickel.

Nickel is known to be a polymorphous metal. The parameters of hexagonal close-packed (hcp) lattice of low-temperature Ni modification that is stable below 380°C are presented in [3], those of Ni face-centered cubic (fcc) modification, in [4]. Probability of hcp Ni occurrence rises in thin-film state. This fact is interpreted in [5] as a phase transition at decreasing film thickness. The transformation is caused by the change of free energy when the surface relative fraction increases. The amorphous structure films have been observed at laser sputtering [6].

Today, there is a considerable interest in Ni films and nanoparticles due to their magnetic and catalytic properties. Formation of metastable hcp phase and non-ferromagnetic behavior of Ni films prepared by pulsed laser deposition have been established [7]. Hexagonal close-packed Ni nanostructures were observed under heteroepitaxial Ni growth on the (001) face of MgO [8]. When lateral size of islands exceeded about 5 nm, the transformation of hcp lattice into ordinary fcc one occurred via martensite mechanism. Ni nanoparticles having both hcp and fcc structure were prepared by complex technological deposition cycles from solutions [9] and by thermal dissociation (dissolution) of organometal precursors [10]. Magnetic properties of Ni nanoparticles corresponded to both paramagnetic and ferromagnetic states.

The aims of this work are to investigate the effects of the substrate temperature and oxygen pressure in evaporating chamber on the structure and phase state of laser Ni film condensates using transmission electron microscopy and to study the mechanisms of structure and phase transformations and magnetic property evolution of films after annealing.

The films have been prepared by pulsed laser deposition of nickel onto KCl (001) single crystal substrates as well as onto KCl substrate coated with an amorphous carbon thin layer. The usual laser deposition method [2] consisting in pulsed sputtering of high purity nickel target in vacuum or in oxygen atmosphere in continuous-flow regime has been used. The laser emission of nanosecond duration and $\lambda = 1.06$ μm wavelength was introduced into vacuum chamber using modulated Q-switch regime and was focused on rotating Ni target. The repetition frequency $\nu = 25$ Hz. The film thickness t was 28 to 30 nm. The film thickness was controlled by the photometric method using reference samples of known thickness. The substrate temperature was varied in the range from 290 to 700 K. The oxygen pressure in vacuum chamber $P(O_2)$ was varied from $5 \cdot 10^{-3}$ to 13.3 Pa.

Annealing of these films in vacuum without stripping off from the substrate activated the structure transformations in the films. For transmission electron microscopy studies the as-prepared films and annealed ones were stripped off from substrates in distilled water and then mounted onto object grids.

The electron diffraction examination and the transmission electron microscopy (TEM) were used for the film structure studies. The EM-100L electron microscope working in electron diffraction regime was used to observe the electron diffraction patterns. The bright-field TEM images of 120000–200000 magnification were obtained using a PEM-100-01 electron microscope. Using these images, the histograms describing the distribution of Ni grain size D were plotted and mean grain size $<D>$ was found.

Magnetic properties of as-prepared nickel films and those annealed at 670–700 K were studied by high sensitive vibrating magnetometer. The hysteresis loops were measured on square-shaped samples of about 1 cm^2 area in magnetic fields up to 1000 Oe applied in the film plane along two perpendicular directions at room temperature. The mean saturation magnetization was determined by comparing signals from reference sample and that under investigation.

It was found that using PLD method, it is possible to initiate the formation of different structure states in films by varying the pressure P in evaporating chamber and the substrate temperature T_S (see Table 1):

i) Amorphous state arises when laser erosion Ni plasma is condensed onto both orienting substrates ((001) KCl) and non-orienting ones (amorphous carbon) at $T_S = 290$ K (Fig. 1a). Annealing of film on substrate in vacuum at $T_a = 710$ K during $\tau_a = 190$ min stimulates its partial crystallization (Fig. 1b). Here, finely dispersed fcc Ni crystals

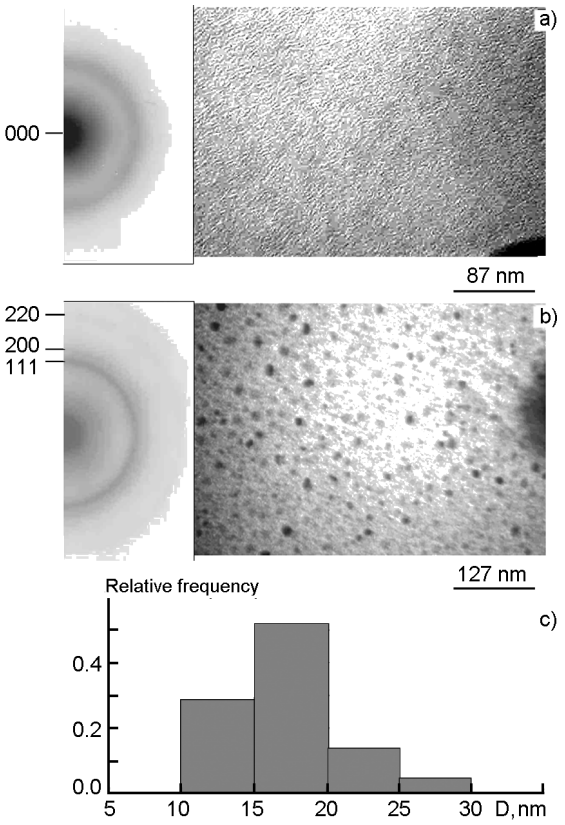

Fig. 1. Pulse laser deposition of Ni films onto (001) KCl substrate: (a) Electron diffraction pattern and TEM image of an amorphous film deposited at substrate temperature T_S = 290 K; (b) The same after annealing of films on the substrate in vacuum at T_a = 710 K during τ_a = 190 min. The electron diffraction pattern contrast is inverted; (c) Histogram of size (D) distribution of Ni particles segregated in amorphous matrix after annealing.

are segregated in amorphous matrix. The size distribution histogram of crystal segregations in amorphous matrix is shown in Fig. 1c. The mean size of segregations $<D>$ = 17.3 nm, the mean distance between segregations $<L>$ = 34.6 nm. More detailed statistical data are in Table.

ii). When the substrate temperature rises in the range of T_S≈350–660 K, the Ni films of metastable hcp structure are formed. Only polycrystalline films were generated on the non-orienting substrates. The electron diffraction pattern and TEM image of hcp Ni film deposited at T_S = 530 K onto KCl substrate coated with amorphous carbon film are shown in Fig. 2a. In accordance with histogram, shown in Fig. 2b, the mean size of Ni grains $<D>$ is 5.0 nm.

Partially oriented films are formed on the orienting substrates. As T_S rises, the extent of film orientation increases. Fig. 3a demonstrates the electron diffraction pattern and TEM image of an hcp Ni film deposited at the same temperature (T_S = 530 K) onto (001) KCl surface. According to histogram shown in Fig. 3b, the mean size of Ni grain increases and amounts 13.2 nm.

The annealing of the investigated hcp Ni films (both polycrystalline and texture-oriented) results in the transition thereof into stable fcc state. The electron diffraction pattern and TEM image of fcc Ni films obtained by annealing of initial hcp Ni ones are shown in Figs. 2c and 3c. Annealing of films on substrates was carried out at T_a = 720 K during τ_a = 150 min. The histograms (Figs. 2d and 3d) illustrate the change of Ni grain size distribution after annealing. In the first case, the mean Ni grain size $<D>$ increased from 5.0 nm to 77.7 nm, in the second one, from 13.2 nm to 71.1 nm (see Table).

iii). The polycrystalline fcc films (deposited onto non-oriented substrates) and epitaxial ones (deposited onto orienting substrates) are formed when deposition is

Table. Annealing effect on structure and statistic characteristics of PLD Ni films

Grain (particles) characteristics	Ni deposition onto (001) KCl. T_S = 290 K		Ni deposition onto amorphous carbon. T_S = 530 K		Ni deposition onto (001) KCl. T_S = 530 K	
	Initial state	Post annealing state	Initial state	Post annealing state	Initial state	Post annealing state
Structure	Amorphous	Amorphous with fcc segregations	hcp polycrystalline	fcc polycrystalline	hcp texture	fcc texture
$<D>$, nm	–	17.3	5.0	77.7	13.2	71.1
τ, nm	–	3.6	1.7	31.7	4.6	27.5
K, %	–	20.8	34.0	40.8	34.8	38.7

Notes. $<D>$ is mean grain (particle) size; σ, standard deviation; K, coefficient of variation $100\sigma/<D>$.

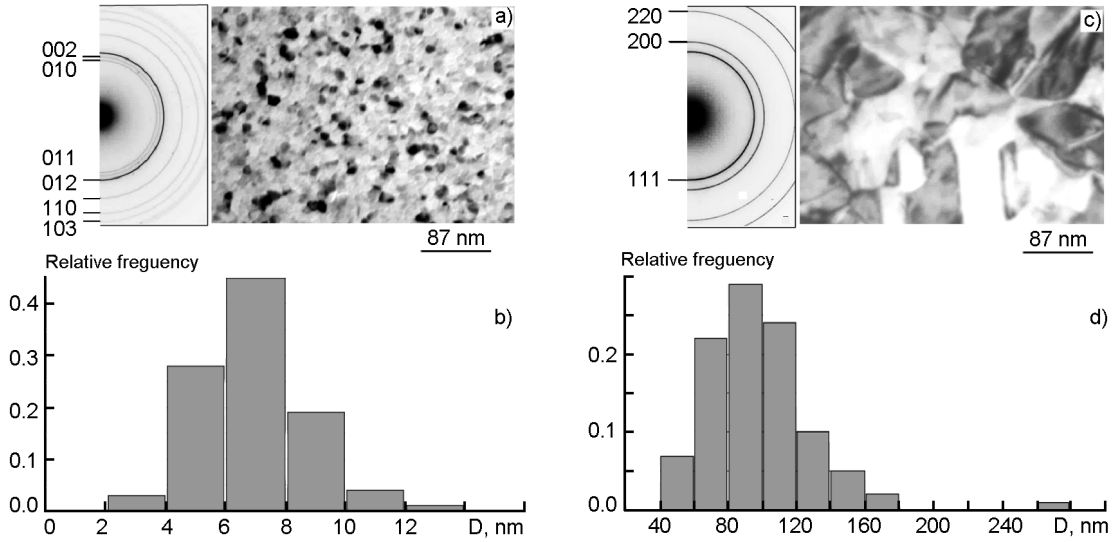

Fig. 2. The hcp → fcc phase transition in Ni films deposited by PLD onto amorphous carbon thin films: (a) Electron diffraction pattern and TEM image of an hcp Ni film deposited at T_S = 530 K; (b) Histogram of size (D) distribution of hcp Ni grains; (c) Electron diffraction pattern and TEM image of Ni film with fcc structure obtained after annealing of initial film on the substrate in vacuum. T_S = 720 K, τ_a = 150 min; (d) Histogram of size (D) distribution of fcc Ni grains.

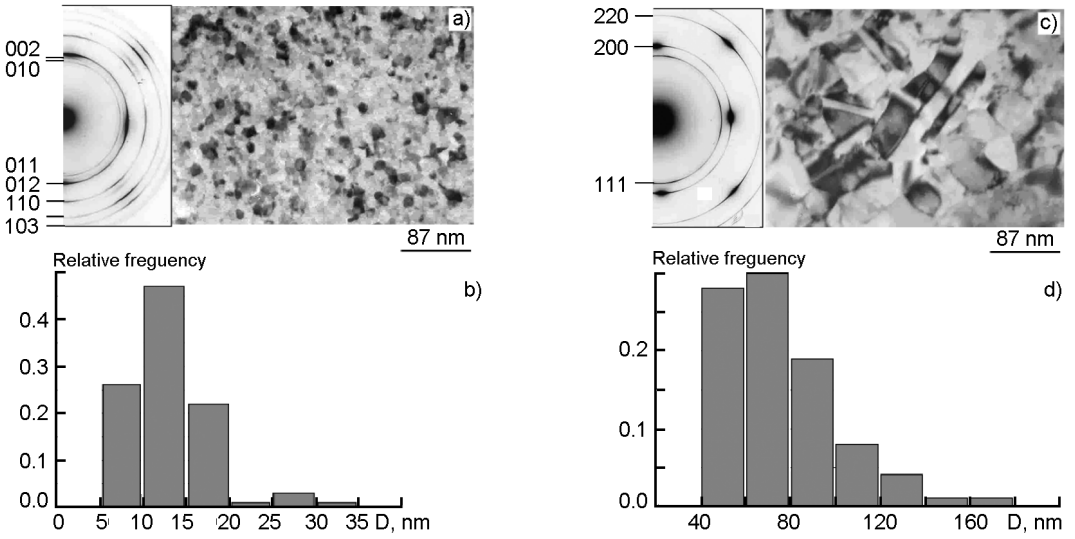

Fig. 3. The hcp → fcc phase transition in Ni films deposited by PLD onto (001) KCl substrate: (a) Electron diffraction pattern and TEM image of an hcp Ni film deposited at T_S = 530 K; (b) Histogram of size (D) distribution of hcp Ni grains; (c) Electron diffraction pattern and TEM image of an fcc Ni film obtained after annealing of initial film on the substrate in vacuum. T_a = 720 K, τ_a = 150 min; (d) Histogram of size (D) distribution of fcc Ni grains.

carried out at substrate temperature T_S = 670–700 K.

The diagram describing the dependence of mean Ni grain size <D> on the deposition temperature T_S is presented in Fig. 4a. In this figure, the mean grain sizes of annealed Ni films are shown, too. The solid line is drawn through points characterizing the grain sizes of as-prepared Ni films. The arrows connect the points corresponding to as-prepared hcp samples and fcc annealed ones. In accordance with the plot, the considerable rise of <D> is accompanied by phase transition of Ni lattice from hcp to fcc state.

iv) At laser sputtering of nickel in oxygen atmosphere under $P(O_2) \geq 0.13$ Pa, NiO oxide phase having fcc polycrystalline structure is formed (Fig. 5).

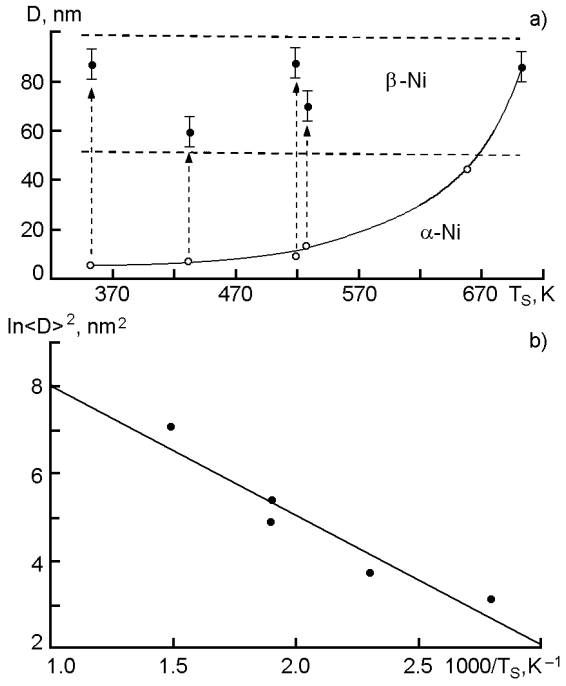

Fig. 4. (a) Dependence of Ni mean grain size $<D>$ on substrate temperature T_S and on post-deposition annealing. The curve is plotted through the points characterizing the Ni grain sizes of as-prepared films. The arrows link together the data corresponding to samples prior to and after annealing, respectively. o — hcp Ni phase. • — fcc Ni phase; (b) Plot for hcp Ni films drawn using $\ln<D>^2$–$1000/T_S$ coordinates.

We have found that as-prepared Ni films having both amorphous structure (Fig. 1a) and metastable hcp one (Figs. 2a, 3a) do not reveal magnetic moment (Figs 6a, 6c, 6e) exceeding the magnetometer sensitivity threshold (corresponding to magnetization value less than 1–5 G for above-mentioned size parameters of samples under investigation) in magnetic fields up to 1000 Oe.

After annealing, the magnetic state of films deposited onto both amorphous carbon layer and (001) surface of KCl substrates changed. Namely, the magnetic moment increases significantly and hysteresis is observed at magnetization reversal (Figs. 6d, 6f). The in-plane anisotropy is absent. Ni films on amorphous carbon substrates are characterized by coercive force $H_C = 80$ Oe and saturation magnetic field $H_S \approx 150$ Oe. For (001) KCl substrates, these values amount of 110 Oe and 150 Oe, respectively. Saturation magnetization values I_S are in the range of 300 to 310 G, being somewhat lower than I_S for bulk nickel (484 G [11]).

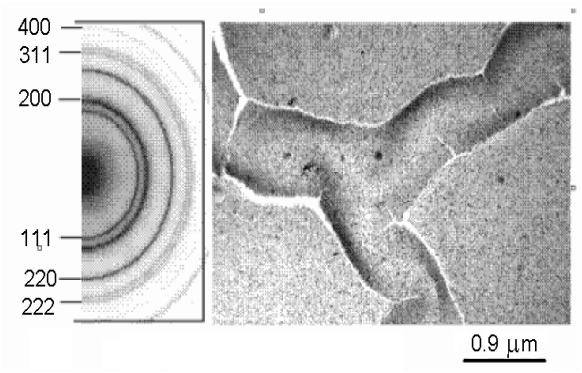

Fig. 5. Electron diffraction pattern and TEM image of an fcc NiO film. PLD was carried out in oxygen atmosphere at pressure $P(O_2) = 1.33$ Pa and substrate temperature $T_S = 290$ K.

The diagram of structure and phase states for laser condensate films of various metals deposited onto unheated substrates under different oxygen pressure values in evaporating chamber is presented in [2, 12]. Our data concerning to structure and phase states of PLD Ni films are shown in the improved diagram (Fig. 7). On the abscissa axis, the values of initial adsorption heat of oxygen onto metal surface, Q_0, are plotted because the film phase state is influenced most strongly by that gas. The Q_0 values for Ni surface are cited in [13]. On the ordinate axis, the values of dimensionless parameter Γ_U are shown. This parameter equals the ratio of gas atomic flux J_2 hitting the growth surface during the pulse repetition period τ to flux J_1 of metal atoms during the deposition pulse time τ_1:

$$\Gamma_U = \frac{\int_0^{\tau} J_2(t)dt}{\int_0^{\varphi_1} J_1(t)dt}. \quad (1)$$

The following areas are marked in the diagram. The area (I) corresponds to crystalline metal. The subarea (1)′ is marked as a particular case (formation of oriented and epitaxial structures under deposition onto alkali halide crystal substrates). The area (II) demonstrates the presence of polycrystalline structures with amorphous component between metal grains. The area (III) corresponds to amorphous structures. The area (IV) belongs to phases with composition close to stoichiometric oxides.

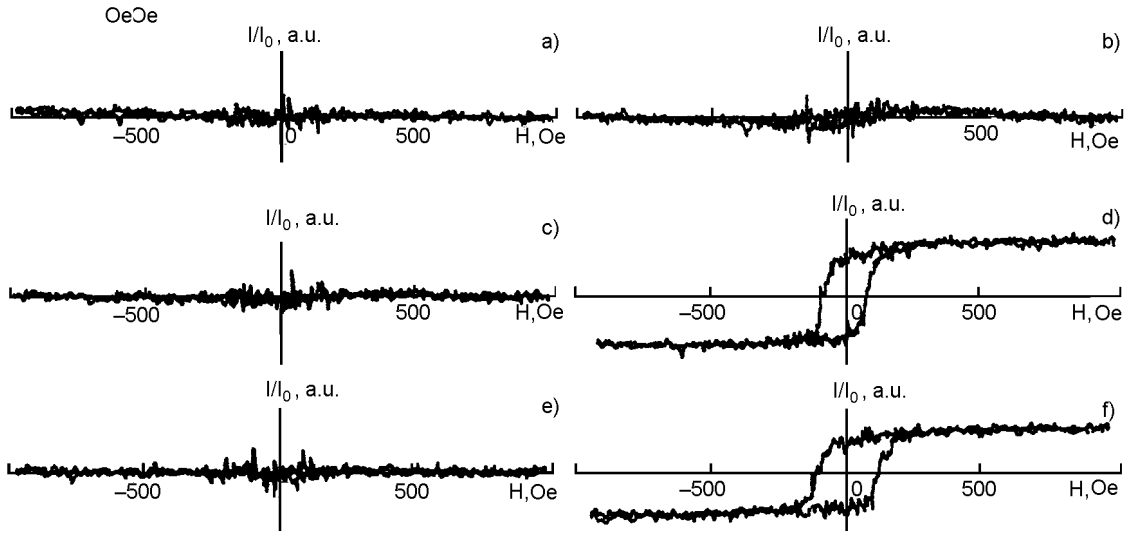

Fig. 6. Magnetization loops of PLD Ni films: (a) Amorphous films (see Fig. 1a) deposited onto KCl (001) surface at T_S = 290 K; (b) The same after partial crystallization (see Fig. 1b) as a result of annealing at T_a = 710 K, τ_a = 190 min; (c) Polycrystalline hcp films (see Fig. 2a) deposited onto amorphous carbon surface at T_S = 530 K; (d) The same after transition to fcc structure (see Fig. 2c) as a result of annealing at T_a = 720 K, τ_a = 150 min; (e) Partially oriented hcp film (see Fig. 3a) deposited onto (001) KCl surface T_S = 530 K; (f) The same after transition to fcc structure (see Fig. 3c) after annealing at T_a = 720 K, τ_a = 150 min.

The structure formed as a result of nickel PLD in oxygen atmosphere at pressure $P(O_2) \geq 0.13$ Pa corresponds to area (IV) (the square in the diagram of Fig. 7). Here, the stoichiometric fcc oxide NiO is generated (see Fig. 5). When the pressure decreases, the amorphous state corresponding to area (III) (the circle in diagram of Fig. 7) is realized. An increasing flux of metal component J_1 initiates the conversion to area (I) (the triangle in the above mentioned diagram). This case is realized in combined laser and thermal co-deposition method when vapor-plasma flux and flux of metal atoms evaporated thermally are deposited on substrate [14].

The dependences of mean grain size $\langle D \rangle$ of hcp Ni vs substrate temperature T_S plotted using coordinates $\ln\langle D \rangle^2 - 1000/T_S$ are shown in Fig. 4b. It follows from this figure that experimental points are situated on straight line described by the equation:

$$\ln\langle D \rangle^2 = a + b\left(\frac{1000}{T_S}\right), \qquad (2)$$

where $a = 11.06$ and $b = -2.99$. On the other hand [15], it is known that the dependence of mean grain size $\langle D \rangle$ of deposited films are allowed to described by exponential function

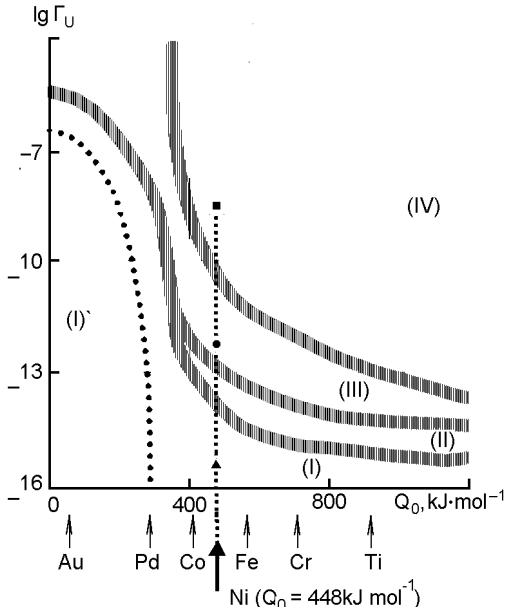

Fig. 7. The structure state diagram of films deposited by pulse laser sputtering of metal targets in oxygen atmosphere.

$$\langle D \rangle^2 = A\exp\left(-\frac{U}{RT_S}\right). \qquad (3)$$

In Eq. (3), A is pre-exponential factor; U is effective activation energy of processes controlling the grain generation. Comparing

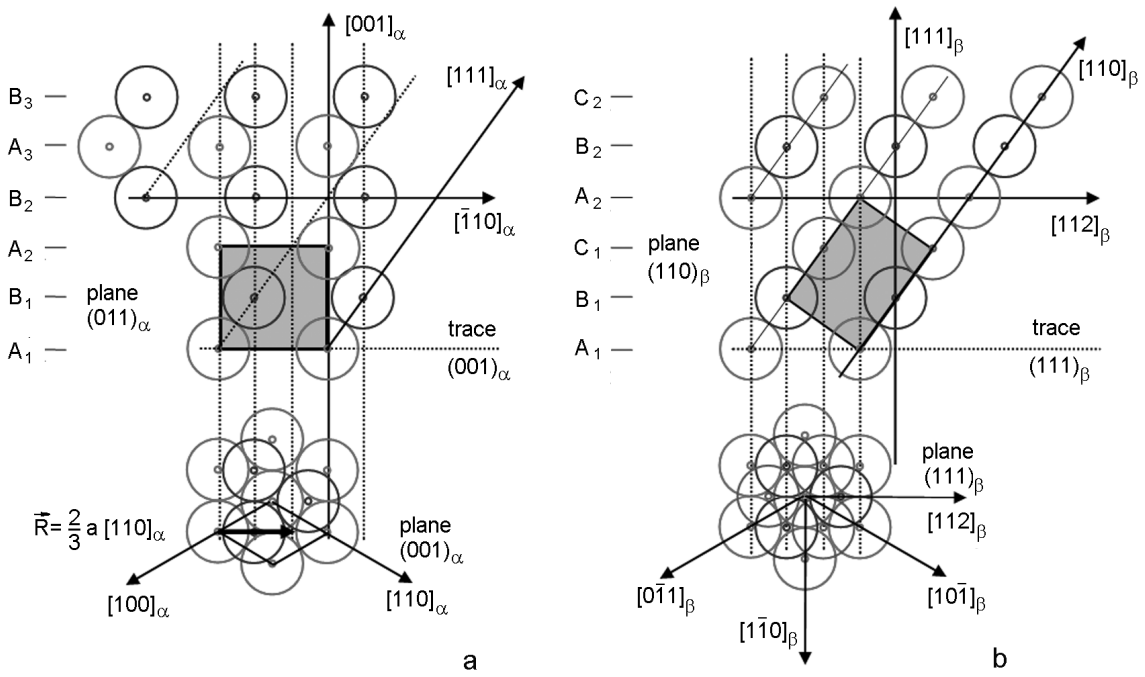

Fig. 8. Schematic model of phase transition from low-temperature hcp modification (α-Ni phase) to high-temperature fcc one (β-Ni phase) in PLD films under annealing: (a) hcp crystal lattice in projections onto (110) and (001) planes. Red and blue circles correspond to atoms in the same type planes of ABAB... sequence; (b) fcc crystal lattice in projection onto (110) and (111) planes. Red, blue, and green circles correspond to atoms of the same type in atomic planes of ABCABC... consequence.

the equations (2) and (3) and using the above-mentioned a and b coefficients, we get $A = 6.4 \cdot 10^{-14}$ (m^2) and $U = 24.86$ kJ/mol (0.26 eV/atom).

According to [15] the typical values of U for pure metals deposited at substrate temperatures T_S not exceeding 0.3 melting point (so-called first condensation zone) are 0.2 to 0.25 eV/atom. It should be concluded that the value of $U = 0.26$ eV/atom determined for Ni in our work agrees satisfactory with literature data.

Annealing of Ni films on (001) KCl substrate in vacuum in temperature range $T_a \approx 710-720$ K activates the recrystallization processes. As a result of recrystallization, the increasing of mean Ni grain size $<D>$ is observed and the phase transformation from low-temperature hcp modification (α-Ni phase) to high-temperature fcc one (β-Ni phase) occurs. To carry out the crystallographic analysis, it is reasonable to use an example of inverse allotropic transformation $\beta \rightarrow \alpha$, which occurs in a martensite manner in Co under sample cooling [16].

Fig. 8a shows the bilayer hcp lattice (α-Ni phase) as a sequence of close-packed atomic layers (ABAB...). The growth of high-temperature β-Ni phase crystal starts from some (001) plane of initial hcp crystal, this plane remaining invariant. We suppose that the first two bottom layers A_1 and B_1 of α-Ni phase (001) planes correspond to the first two bottom layers A_1 and B_1 of β-Ni phase (111) planes. When ($A_2B_2A_3B_3$) layers of (001) α-Ni phase are shifted by vector $\mathbf{R} = 2/3\ a[\bar{1}10]$, then A_2 and B_2 planes of bilayer stacking pass into (111) C_1 and A_2 of three-layered stacking. Next similar shifts stimulate the following transition: $A_3 \rightarrow B_2$ and $B_3 > C_2$ etc. In this way, the reconstruction of lattice from bilayer stacking to three-layered one occurs.

The change of film magnetic moment resulting from annealing that we have established can be explained as follows. The annealing stimulates the transformation of Ni crystal structure from metastable hcp one (α-Ni phase) to equilibrium fcc phase (β-Ni phase). A model is known describing the transition metal electron structure [17]. In that model, the hcp Ni would not have a spontaneous magnetization while the fcc Ni is ferromagnetic. In this case, the magnetic properties changes after annealing are due to magnetic phase transformation.

There are contrary viewpoints, too. In [18], it has been shown that hcp Ni is ferromagnetic and its atomic magnetic moment is equal to 0.59 μ_B, being somewhat less than atomic magnetic moment of stable fcc phase (0.60μ_B). However, in nanodispersed thin film systems where the grains are sufficiently small and isolated from each other (volume concentration of magnetic phase is lower than 30 %), the superparamagnetism may be observed. As a consequence, the magnetic moment of the sample under investigation will be very small in the applied magnetic fields (<1000 Oe). This case takes place in amorphous-crystalline Ni films (see Fig. 1b and Fig. 6b) where fcc grains of β-Ni phase are embedded into amorphous nonferromagnetic matrix. Using data of Fig. 1 and Table, the mean grain size and mean intergrain distance have been evaluated to bes $<D>$ = 17.3 nm and $<L>$ = 34.6 nm, respectively. According to [19], an increase of $<D>$ and a decrease of $<L>$ may initiate the transition from the superparamagnetic state to ferromagnetic one.

The hcp α-Ni films deposited onto amorphous carbon substrates and (001) KCl ones are characterized by fine-grain polycrystalline structure ($<D>$ = 5–13 nm) and by absence of any observable magnetic moment. However, TEM micrographs shown in Figs. 2a and 3a demonstrate a close grain contact and absence of grain interlayers. The latter confirms the supposition that the changes in magnetic properties after annealing are due to magnetic phase transformation.

Thus, to conclude, variations of oxygen pressure in the vacuum chamber and of substrate temperature during Ni PLD process provide a wide variety of thin film states, including the amorphous Ni films, metastable hcp Ni (α-Ni phase), stable fcc Ni (β-Ni phase) and fcc Ni oxide. The effective activation energy of processes controlling the formation of α-Ni phase grains amounts about 0.26 eV/atom. Annealing of amorphous films activates their crystallization going with formation of off-oriented segregations of β-Ni phase. Annealing of metastable hcp Ni films initiates the hcp → fcc polymorphous transition followed by sharp increasing of grain size and change of film magnetic characteristics. As a result of annealing, the films take a noticeable magnetic moment and hysteresis takes place at magnetization reversal.

Reference

1. E.E.Shalygina, L.V.Kozlovsky, N.M.Abrosimova, M.A.Mukasheva, *Fiz. Tverd. Tel*a 47, 660 (2005).
2. A.G. Bagmut, V.M. Kosevich, G.P. Nikolaichuk et al., *Functional Materials* 6, 75, (1999).
3. International Centre for Diffraction Data - JCPDC, 1996, card № 45-1027.
4. International Centre for Diffraction Data - JCPDC, 1996, card № 04-0850.
5. A.I.Bublik, B.Ya.Pines, Dokl. AN SSSR 87, 215 (1952).
6. S.N.Tarasenko, *Fiz. Khim. Obrab. Mater.* No. 3, 76, (1989).
7. S.M.Zharkov, V.S.Zhigalov, G.I.Frolov, *Fiz. Metal. Metalloved*. 81, 170 (1996).
8. W. Tian, H.P.Sun, X.Q. Pan et all., *Applied Physics Letters*, 86, 13915-1 (2005).
9. Yoon Tae Jeon, Je Yong Moon, Gang Ho Lee et all., *J. Phys. Chem.* 110, 1187 (2006).
10. Yuanzhi Chen, Dong-Liang Peng, Dongxing Lin, Xiaohua Luo, *Nanotechnolology* 18, 1 (2007).
11. R. Bozort. Ferromagnetism, Izd. Inostr. Liter., Moscow (1956) [Russian edition is cited].
12. A.G.Bagmut, *Poverkhnost': Roentgen., Sinkhrotron. Neutron Issled.* No. 6, 65 (2008).
13. Ya.D.Kogan, B/F/Kolachev, Yu.V.Levinsky et al., Metal/Gas Interaction Constants: A Reference Book. Metallurgia, Moscow (1987) [in Russian].
14. A.G. Bagmut, V.M. Kosevich, G.P. Nikolaichuk, *Fiz. Khim. Obrab. Mater.* No. 3, 74 (1988).
15. B.A.Movchan, I.S.Malashenko. Vacuum-Deposited Refractory Coatings. Naukova Dumka, Kiev (1983) [in Russian].
16. Ya.S.Umansky, Yu.A.Skakov. Physics of Metals. Atomizdat, Moscow (1978) [in Russian].
17. J.Gudinaff. Band structure of transition d-metals and alloys thereof. Izd. Inostr. Liter., Moscow (1963) [Russian edition is cited].
18. X. He, L.T. Kong, B.X. Liu, *J. Appl. Phys.* 97, 106107 (2005).
19. A. Frydman, T.L. Kirk, R.C. Dynes, *Solid State Communs.* 114, 481 (2000).

Структурно-фазові стани та зміна магнітних властивостей при рекристалізації тонкоплівкових лазерних конденсатів нікелю

О.Г.Багмут, І.Г.Шипкова, В.А.Жучков

Проведено електронно-мікроскопічне дослідження впливу температури підкладки та тиску кисню у випарній камері на структуру та фазовий склад лазерних конденсатів нікелю. Вивчено закономірності структурно-фазових трансформацій та зміни магнітних властивостей плівок після відпалу. Установлено, що варіювання тиском кисню у випарній камері й температурою підкладки у процесі конденсації нікелю забезпечують широкий спектр тонкоплівкових станів. Формуються аморфні плівки Ni, плівки Ni з метастабільною ГПУ решіткою (α фаза), плівки Ni зі стабільною ГЦК граткою (β фаза) і плівки оксиду Ni зі структурою ГЦК. Ефективне значення енергії активації процесів, що контролюють утворення зерен α фази Ni, становить ~ 0,26 еВ/атом. Відпал аморфних плівок ініціює їхню кристалізацію з утворенням розорієнтованих виділень β фази нікелю. Відпал плівок Ni з метастабільною ГПУ граткою ініціює поліморфне перетворення ГПУ > ГЦК, що супроводжується різким збільшенням розміру зерен і зміною магнітних характеристик плівки. У результаті відпалу плівки набувають магнітного моменту, а при перемагнічуванні має місце гістерезис.